Exp Fluids (2008) 44:773–780
DOI 10.1007/s00348-007-0433-9

RESEARCH ARTICLE

A method for estimating wall friction in turbulent wall-bounded flows

Anthony Kendall · Manoochehr Koochesfahani

Received: 16 March 2007 / Revised: 27 July 2007 / Accepted: 30 October 2007 / Published online: 30 November 2007

Abstract We describe a simple method for estimating turbulent boundary layer wall friction using the fit of measured velocity data to a boundary layer model profile that extends the logarithmic profile all the way to the wall. Two models for the boundary layer profile are examined, the power-series interpolation scheme of Spalding and the Musker profile which is based on the eddy viscosity concept. The performance of the method is quantified using recent experimental data in zero pressure gradient flat-plate turbulent boundary layers, and favorable pressure gradient turbulent boundary layers in a pipe, for which independent measurements of wall shear are also available. Between the two model profiles tested, the Musker profile performs much better than the Spalding profile. Results show that the new procedure can provide highly accurate estimates of wall shear with a mean error of about 0.5% in friction velocity, or 1% in shear stress, an accuracy that is comparable to that from independent direct measurements of wall shear stress. An important advantage of the method is its ability to provide accurate estimates of wall shear not only based on many data points in a velocity profile but also very sparse data points in the velocity profile, including only a single data point such as that originating from a near-wall probe.

1 Introduction

A common approach for estimating the wall shear stress, τ_w, in turbulent boundary layers is the Clauser method (Clauser 1956; Fernholz and Finley 1996). In this method, measurement of the mean velocity profile $U(y)$ is used to estimate the friction velocity $u_\tau \equiv \sqrt{\tau_w/\rho}$ using the fit of the measured data to the logarithmic region of the boundary layer, given by

$$\frac{U(y)}{u_\tau} = \frac{1}{\kappa}\ln\left(\frac{y\,u_\tau}{\nu}\right) + B. \quad (1)$$

There are several aspects in the implementation of this method that can introduce uncertainties in the estimated shear stress. One needs to select the beginning and ending points within the data set that are believed to fall within the log-linear region, and this brings an element of user subjectivity into the result. A more important aspect, however, is the fact that the estimate of friction velocity is directly related to the choice for the von Kármán constant κ. Different values of this constant are often reported in the literature (Zanoun et al. 2003), and a number of studies have indicated that the Clauser method produces artificially high friction velocities, especially at the low range of Reynolds numbers (Kline et al. 1967; Blackwelder and Haritonidis 1983; Spalart 1988; Ong and Wallace 1998; Wei et al. 2005). For example, the friction velocity estimated from the Clauser method was reported to have an error varying between 8 and 20% over a Reynolds number in the range of Re_θ = 1,000–10,000 (Blackwelder and Haritonidis 1983). At very high Reynolds numbers, the larger extent of a well-developed log-linear region improves the accuracy of the Clauser method as long as a suitably accurate value of κ is used. A related approach introduced by Coles (1968) extends the logarithmic velocity profile towards the freestream by incorporating the wake function. In this approach, the data points near the wall are not utilized; in particular, the data in the region $y^+ \equiv yu_\tau/\nu < 50$ are specifically excluded (Coles 1968).

A. Kendall · M. Koochesfahani (✉)
Department of Mechanical Engineering,
Michigan State University,
East Lansing, MI 48824, USA
e-mail: koochesf@egr.msu.edu

Another approach for wall-shear estimation is to rely on velocity measurements that are carried out by fine probes very close to the wall in the linear sublayer. Advances in microsensors, for example, have led to flush surface-mounted optical probes that provide single-point samples of the velocity as close as 70 μm from the wall (Fourguette et al. 2001, 2003). Hot-wire velocity measurements have been carried out down to 35 μm away from the wall in turbulent boundary layers (Österlund 1999). The challenge in utilizing the near-wall velocity data for wall shear estimation is that in a typical measurement the actual location of the velocity information in wall units is not known a priori and, depending on the flow Reynolds number, it may not occur in the linear sublayer, but in the logarithmic region, or in the buffer layer joining these two regions.

The method we describe here was initially motivated by the need to estimate the wall-shear stress based on near-wall single-point, or very sparse, velocity data for which the previously described methods would not be helpful. Because of the expectation that modern probes are able to obtain more velocity data closer to the wall as opposed to data closer to the freestream, the method we present utilizes the fit of the measured data to a boundary layer model profile that extends the logarithmic profile all the way to the wall. This methodology was originally devised several years ago to extract wall-shear information from single-point data obtained from surface-mounted optical MEMS-based probes (Fourguette et al. 2003). In this paper, we present a quantitative assessment of the performance of the method using recent experimental data in zero pressure gradient flat-plate turbulent boundary layers, and favorable pressure gradient turbulent boundary layers in a pipe, for which independent measurements of wall shear are also available. Even though the original motivation of our method was to address the case of near-wall probes with sparse data points, the approach can equally be used in cases where a full survey of boundary layer profile with many data points is available. In the latter case, the approach we present takes advantage of all the velocity data available down to the wall for estimating wall shear and does not rely only on the data in the log-linear region as in the Clauser method.

In the sections that follow, we describe the method for estimating the wall shear stress and give a brief account of the experimental database used to assess its performance. The performance of the method is characterized using both many data points in a velocity profile and also very sparse measurements such as single-point data. We will show that in both cases the new procedure can provide highly accurate estimates of the wall shear with a mean error of about 0.5% in friction velocity, or 1% in shear stress. This accuracy is comparable to that from independent direct measurements of wall shear stress.

2 Experimental database and wall-shear estimation method

2.1 Experimental database

The velocity measurements of Österlund (1999) and Österlund et al. (2000) provide the primary database for assessing the performance of the method we describe in this paper. This database consists of 70 mean velocity profiles of a zero pressure gradient 2-D turbulent boundary layer measured with hot-wire anemometry at different freestream velocities and downstream locations along a flat-plate, covering a Reynolds number in the range $2{,}533 < Re_\theta < 27{,}320$. For each case, the value of wall shear τ_w is available based on a skin-friction relation developed from independent oil-film interferometry measurements. The accuracy of wall-shear data is reported to be 1% (corresponding to 0.5% accuracy in friction velocity u_τ).

The second database is the favorable pressure gradient superpipe boundary layer data of McKeon et al. (2004). The finest Pitot probe (0.3 mm diameter) database is used here and it comprises of 19 mean velocity profiles spanning a pipe Reynolds number range $7.43 \times 10^4 < Re_D < 3.57 \times 10^7$. The wall-shear stress is determined from pressure gradient measurements over a known length of pipe with an accuracy better than 0.8% (accuracy improves at lower Reynolds numbers).

2.2 Models of mean boundary layer profiles

Two models of turbulent boundary layer mean velocity profile are evaluated in this work. The first is the profile of Spalding (1961), which is a power-series interpolation scheme joining the linear sublayer to the logarithmic region. The Spalding profile has the following form

$$y^+ = u^+ + \exp(-\kappa B)\left[\exp(\kappa u^+) - 1 - \kappa u^+ - \frac{(\kappa u^+)^2}{2} - \frac{(\kappa u^+)^3}{6}\right], \quad (2)$$

where the usual inner variable normalization is used, i.e. $y^+ = (y - y_0)u_\tau/\nu$ and $u^+ = U/u_\tau$. In these expressions, U is the mean velocity, ν is the fluid kinematic viscosity and y_0 is retained as the wall coordinate to allow for the possibility of uncertainty in wall location. Throughout this work, we consider the fix set of commonly-used boundary layer constants ($\kappa = 0.41$, $B = 5.0$). Observations of the potential influence of other recently reported values of these constants (Österlund 1999; Österlund et al. 2000) on our conclusions will be discussed at the end of this paper.

The second profile is that due to Musker (1979) and it was suggested to us by Professor Donald Coles of Caltech.

The Musker profile is based on the eddy viscosity model and is given by the solution to the following implicit relation

$$\frac{du^+}{dy^+} = \frac{\frac{(y^+)^2}{\kappa} + \frac{1}{s}}{(y^+)^3 + \frac{(y^+)^2}{\kappa} + \frac{1}{s}}. \quad (3)$$

The variable s is solved for by matching the solution $u^+(y^+)$ from the above equation to the log-linear region (i.e. Equation 1) at sufficiently large y^+. Using an iterative procedure, for the selected boundary layer constants ($\kappa = 0.41$, $B = 5.0$) we find $s = 0.001093$, consistent with previous results in Musker (1979). In our work, we use a discrete form of the velocity profile, a table of velocity data at a set of finely-spaced discrete locations, that is obtained by the integration of Equation (3).

We note that the model profiles we have selected do not include the wake component of the full boundary layer profile. As will be shown, based on the tested cases, highly accurate estimates of wall shear can be obtained with our method of implementation. If needed, the approach can certainly be extended by incorporating appropriate models of the wake component.

The Spalding and Musker profiles are plotted in Fig. 1 along with two of the measured velocity profiles from the Österlund database. By construction, both Spalding and Musker profiles agree in the linear sublayer and logarithmic regions. They differ slightly, however, in the transition between these two regions where the Musker profile has a higher velocity. Note that the Musker profile provides a better fit to the two measured profiles shown here.

2.3 Procedure for friction velocity estimation

For a given measured data set, the velocity points $U(y)$ in real units are normalized into wall units $u^+(y^+)$ by selecting the value of friction velocity u_τ and wall location y_0 that best fit the normalized data against the model profile (i.e. either Spalding or Musker profile). This process is illustrated graphically in Fig. 2 for a particular measured data set (Österlund data set SW981005A, $Re_\theta = 12{,}633$). In this case, y_0 was set to zero since the Österlund database is already referenced to the actual wall location. Figure 2 shows the normalized data in wall units for different iterations on the guess for the friction velocity until the normalized data collapse onto the Musker profile. The iteration sequence was $u_\tau = 0.5$, 1.0, 0.71, 0.79, and 0.75 m/s. For reference, the directly measured value of friction velocity was $u_\tau \approx 0.749$ m/s for this case, illustrating this procedure can provide a highly accurate estimate of wall shear. It can be noted in this figure that an error in the u_τ estimate by much less than 5% is very easily discernible to even simple visual inspection. It is also clear that the same procedure would work very well with very few data points on the profile, even with one single measurement point.

The process just described can, of course, be automated by minimizing the difference between the normalized measured data and the model profile using a least squares procedure. Two different residual functions defining this difference were considered as defined below.

$$\Phi_1 = \frac{1}{N}\sum_{i=0}^{N}\sqrt{(u_i^+(\text{data}) - u_i^+(\text{model}))^2} \quad (4)$$

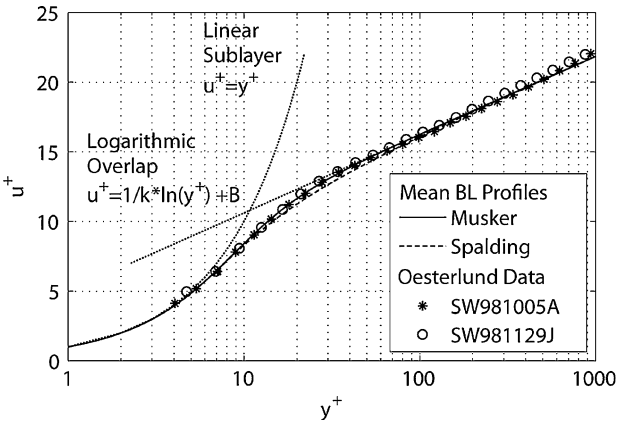

Fig. 1 Comparison of Musker and Spalding profiles ($\kappa = 0.41$, $B = 5$) with two profiles from the Österlund data set (SW981005A, $Re_\theta = 12{,}633$; SW981129J, $Re_\theta = 10{,}162$)

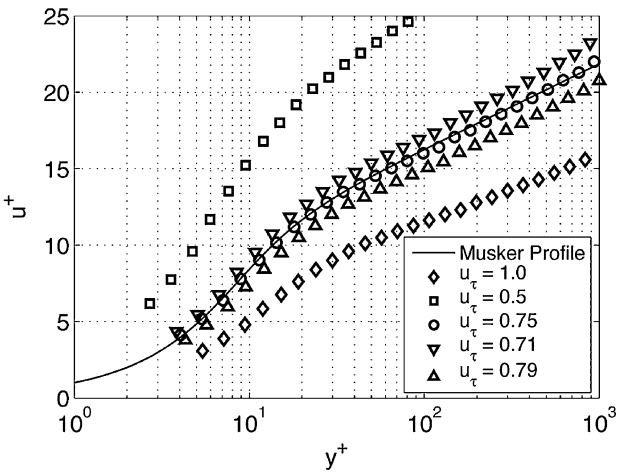

Fig. 2 Illustration showing the iterative determination of friction velocity from a measured profile (Österlund data set SW981005A, $Re_\theta = 12{,}633$)

$$\Phi_2 = \frac{1}{N}\sum_{i=0}^{N}\frac{|\,u_i^+(\text{data}) - u_i^+(\text{model})\,|}{u_i^+(\text{model})}. \quad (5)$$

In these expressions, u_i^+(data) corresponds to the N measured velocity points in wall units located at y_i^+ which are obtained from the measurements in real units using a guess for the value of u_τ, and u_i^+(model) refers to the corresponding model velocities (from Spalding or Musker profile) at those locations. The index i runs from 0 to N because the point ($y_0^+ = 0$, $u_0^+ = 0$) was added in order to enforce the no-slip boundary condition. The residual function Φ_2, which is defined based on a *fractional* difference between points on the data and model profiles, was found to offer an advantage as will be described later.

A two-parameter optimization routine written in MATLAB is used to determine the set of u_τ and y_0 values that minimize the residual function for each of the measured profiles in the data sets of Österlund flat-plate boundary layer data and McKeon et al. superpipe data. The measured data are provided in real units, along with an initial user-specified search domain in the two-parameter space. The search domain is iteratively refined until u_τ and y_0 converge to within a user-defined tolerance level. In the results presented here, the tolerance levels were selected to be 0.0001 m/s for u_τ (better than 0.05% for all cases) and 10 μm for y_0 for cases where wall location was considered variable. Figure 3 shows an example of a shaded contour map of the residual function obtained with this process for one particular data set. Note that it is a smooth surface with a well-defined global minimum corresponding to the values of u_τ and y_0 that provide the best fit to the model profile. We further note that the residual function is less sensitive to y_0 variation than to u_τ (note the abscissa is logarithmic). Thus, convergence in y_0 is generally slower than that in u_τ.

For each data set, the accuracy of the estimated friction velocity u_τ(estimated) from the optimization routine is evaluated by its comparison with the actual measured value u_τ(measured). The resulting percentage error defined by $\delta_{u\tau} = [u_\tau(\text{estimated}) - u_\tau(\text{measured})]/u_\tau(\text{measured})$ provides an ensemble of performance data composed of 70 samples corresponding to the 70 velocity profiles in the Österlund database, and 19 samples for the McKeon et al. superpipe data. The mean and rms errors calculated from this ensemble form the basis of our discussion in the next section.

3 Results and discussion

3.1 Friction factor estimate based on full profile data

We will first consider the situation where all the data from a measured velocity profile are available for estimating the friction velocity. One parameter that needs to be selected is the largest y^+ value, $y^+_{\max}$, that should be used in the optimization process (i.e. only data points with $y_i^+ \le y^+_{\max}$ will be included in the optimization.). This parameter affords one the choice to exclude the portion of the data that might fall in the wake part of the profile. Note that u_τ is not known prior to optimization; therefore, we estimate the optimum u_τ across a range of $y^+_{\max}$ values and then sort out the results afterwards for presentation.

Figure 4 depicts an example of the histogram of error in the friction factor estimate, $\delta_{u\tau}$, for all 70 Österlund data sets based on the fit to the Musker profile and the $y^+_{\max}$ cutoff set to $y^+_{\max} = 500$. As before, y_0 was set to zero since the Österlund database is already referenced to the actual wall location. The important result is that all the errors are quite

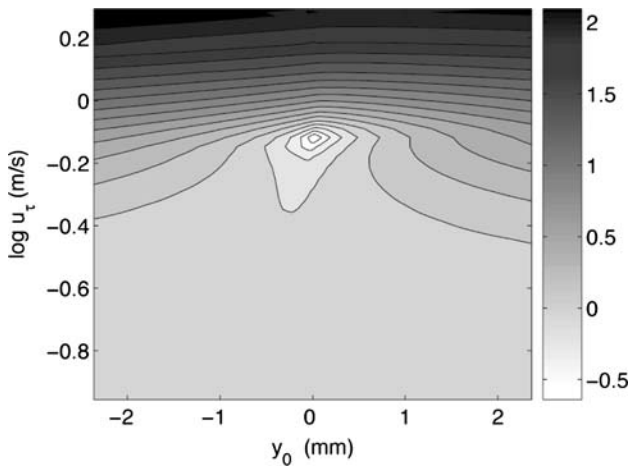

Fig. 3 Shaded contour map of the log of residual Φ_1 versus u_τ and y_0 for the fit of a measured profile (Österlund data set SW981005A, Re_θ = 12,633) to Musker profile

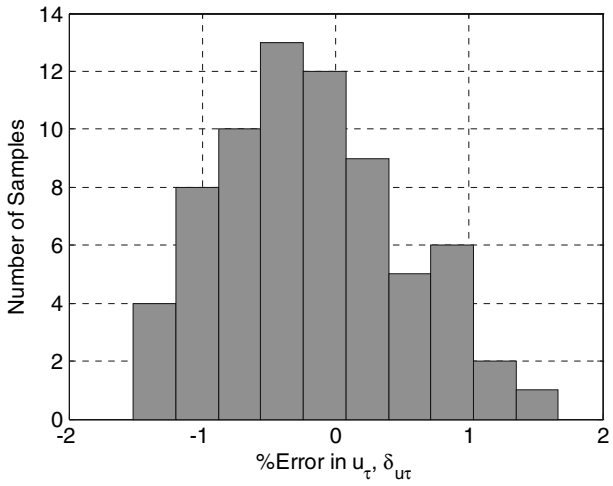

Fig. 4 Histogram of % error in friction velocity for all Österlund data sets using the Musker profile and Φ_2 (y_0 fixed at zero, $y^+_{\max}$ = 500)

low and fall between −1.5 and 1.75% regardless of the Re_θ value of the data. The estimation of friction velocity in this case has a mean error of about −0.25% and an rms error of about 0.75%.

We now compare the performance of the two-model profiles of Musker and Spalding as a function of the y^+_{max} cutoff selected in the optimization. Results are presented in Fig. 5 in terms of the mean and rms error in the estimated friction velocity. For this comparison, the residual function Φ_1 was used and y_0 was set to zero. We note that the Musker profile generally produces a lower mean error overall and is significantly better in the range $20 \leq y^+_{max} \leq 100$. This range of y^+ values corresponds to the transition region between the linear sublayer and the log-linear region. It was already noted in Fig. 1 that Musker profile fits the data more closely in this region than Spalding profile. Because of this better performance, Musker profile is used to obtain the results presented from here on. We note the remarkable accuracy with which the friction factor is estimated over a large range of y^+_{max} cutoff values, with a mean error that is better than 0.5% in friction velocity (or 1% for shear stress).

Figure 5 also illustrates that the mean and rms errors start to increase noticeably at large values of y^+_{max} cutoff, an effect that is caused by the increased number of profiles in the data set that have data points that fall in the wake component of the boundary layer profile. We note that the outer limit of the log region and the start of the wake component move to higher y^+ values with increasing Reynolds number, resulting in higher values of y^+_{max} cutoff becoming effective as Reynolds number increases. Since the deviation of the wake component data points from the model profiles evaluated here leads to residuals that start to become very large in magnitude at large values of y^+_{max} cutoff (results not shown here), an automated procedure can be devised based on the sudden rise of the residual function to limit the y^+_{max} cutoff value for accurate estimate of wall shear. Another approach would be to extend the model profile to include the wake component. A third alternative would be to consider another form of residual function that reduces the sensitivity to the wake component data. The latter alternative is evaluated below.

The detrimental influence of the portion of data within the wake component can be reduced by defining a different residual function Φ_2 that is based on the *fractional* difference between points on the data and model profiles (see Equation 5). Results based on the minimization of Φ_2 are shown in Fig. 6 in comparison with those based on the original Φ_1. It can be seen that the effect of the velocity measurements at large values of y^+ is significantly reduced with a net effect that the friction factor can now be estimated more accurately over a much larger range of y^+_{max} cutoff values, even after the wake component starts to deviate from the logarithmic region. Note, for example, the noticeable reduction in both the mean and rms errors at the highest value of y^+_{max} cutoff shown in Fig. 6. The important observation is that wall shear can be estimated very accurately from mean velocity measurements over a large rage of y^+_{max} cutoff values with a mean error that is better than 0.5% in friction velocity (or 1% for shear stress), an accuracy comparable to that from direct measurements of wall shear stress.

In all the results discussed so far y_0 was fixed at zero since the Österlund database is already referenced to the actual wall location (known to ±5 μm). The ability of the optimization routine to recover non-zero wall locations was

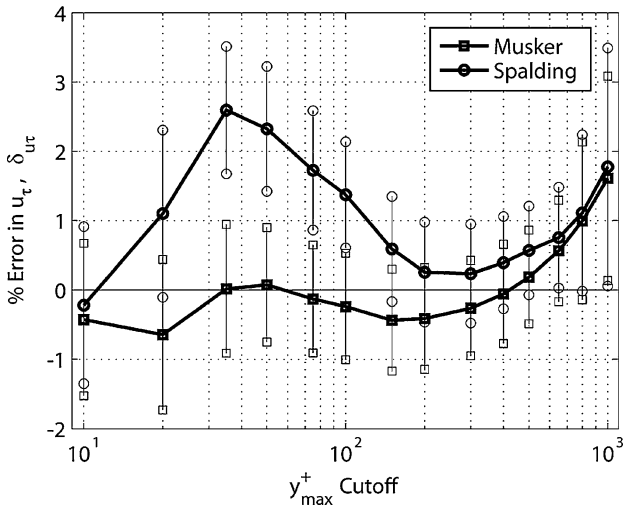

Fig. 5 Comparison of the performance of Musker and Spalding profiles based on the mean and rms of % error in friction velocity for Österlund data (y_0 fixed at zero, residual function Φ_1)

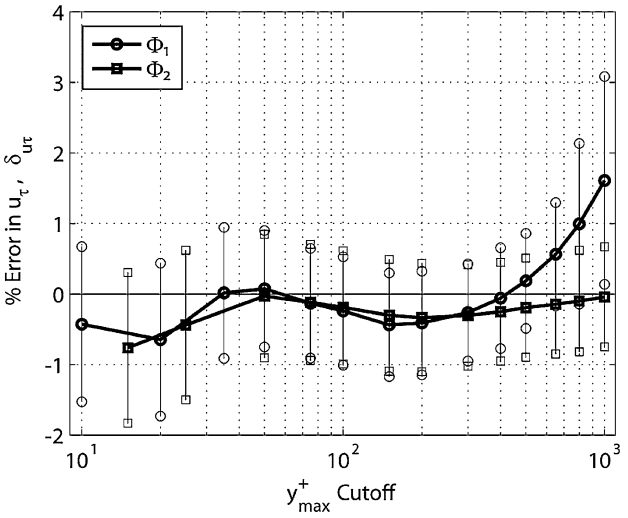

Fig. 6 Comparison of the performance of different residual functions Φ_1 and Φ_2 based on the mean and rms of % error in friction velocity for Österlund data (Musker profile, y_0 fixed at zero)

tested by deliberately offsetting several of the Österlund data sets in the y direction by 40 μm. The optimization routine recovered this offset to an accuracy of approximately ±2 μm in the range $100 < y^+_{max} < 1000$ (in this case, the tolerance for determining y_0 was lowered to 1 μm). The optimization routine was performed a second time on the entire Österlund database, allowing for (possible) non-zero y_0 in the reported data. The mean wall location that was recovered was within the ±5 μm reported accuracy of the actual wall location. Allowing for the possibility of a non-zero wall location in the search routine had only a minor influence on the estimated values of friction factor (about 0.25%).

The performance of the new method was also assessed for estimating wall shear in turbulent boundary layers with non-zero pressure gradient by utilizing the favorable pressure gradient superpipe boundary layer data of McKeon et al. (2004). Results (see Fig. 7) confirm that the method is equally effective in this case as well and the wall shear can be estimated very accurately over a large rage of y^+_{max} cutoff values. Note in this figure that the range of y^+_{max} cutoff values has increased by about an order of magnitude compared to Fig. 6 as a result of the higher Reynolds number of the superpipe data and favorable pressure gradient. It should also be noted that the number of superpipe profiles that contain velocity data at the lower range of y^+ values is less than the total sample size of 19, reducing the actual sample size for calculating the results for lower values of y^+_{max} in Fig. 7. For example, the sample size was 7 (out of the possible 19) for the lowest y^+_{max} value depicted in Fig. 7 and continuously increases to 19 at $y^+_{max} = 2000$.

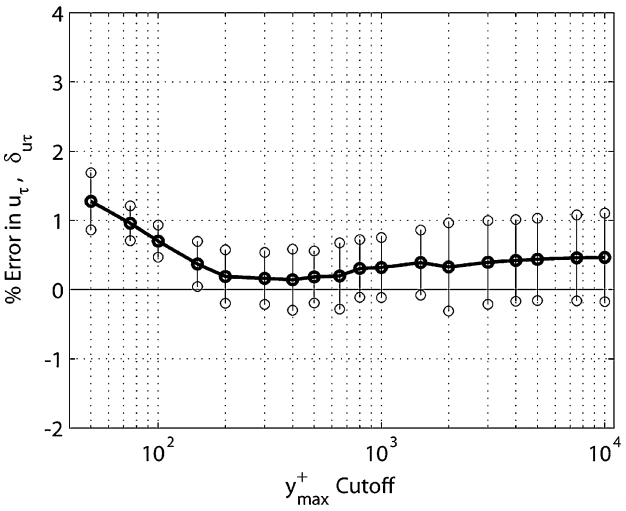

Fig. 7 Mean and rms % error in friction velocity for the McKeon et al. superpipe data (Musker profile, y_0 fixed at zero, residual function Φ_2)

3.2 Friction factor estimate based on sparse data (1-, 2-, and 3-point data)

We now discuss the accuracy of friction velocity estimates based on very sparse data. In particular, we are interested in the case where there is only one mean velocity data point measured at an arbitrary location close to the wall. For example, this would be the case for the optical probe described in AIAA Paper Nos. AIAA-2003–0742 and AIAA-2001–2982 by Fourguette et al., which is designed to obtain single-point velocity data at about 70 μm away from the wall.

Single-point data were extracted from the Österlund data set in the following manner. A nominal y location was first chosen in real units (e.g. y = 50, 75, 100 μm, etc.) to correspond to the location of a hypothetical measurement probe. Since the measured data sets do not necessarily contain data at these exact locations, instead of interpolating the data, we chose to select the nearest actual data points to these nominal locations. The criterion used was that if there were no data points within 10% of the nominal y locations, that data set was excluded from the analysis. The spatial density of data in the Österlund database is high enough that only a few cases were excluded from this analysis. The exception was the lowest location y = 50 μm, for which less than half of the data sets were actually used. The maximum probe location selected was arbitrarily set at y = 7000 μm (i.e. 7 mm) which is significantly higher than the typical location of a near-wall probe.

The motivation for also evaluating a sparse multi-point data scenario derives from the observation that results based on single-point near-wall data are directly affected by the accuracy of both the velocity measurement and the actual location of the measurement relative to the wall. Two-point data is the minimum requirement for determining both friction velocity and wall location y_0 independently. Additional velocity data can further reduce the sensitivity of the estimated wall friction on the accuracy of a single near-wall data point. In this work, we consider two- and three-point data scenarios. In these cases, the first data point was at location y indicated earlier for the single-point case and the locations of the additional velocity data were arbitrarily selected to be at $y_2 = 2y$ and $y_3 = 3y$, simulating a hypothetical two- or three-probe measurement device. As before, instead of interpolating the Österlund data we chose to select the nearest data points to these nominal locations using the same criterion described earlier. In the multi-point analysis, the maximum location of the first probe was selected such that the maximum location of the point farthest away from the wall stayed below an arbitrarily-selected large value (8 mm for 2-point and about 5 mm for 3-point data).

Figure 8 shows the mean % error in the friction velocity estimated based on sparse data. Note that the % error is plotted here on an expanded scale compared to previous plots and, for multi-point cases, the y location in this figure refers to the location of the first data point closest to the wall. The most important conclusion from Fig. 8 is that we can obtain a highly accurate estimate of friction velocity with only a single data point. The corresponding values of mean error are comparable to those obtained earlier based on the full-profile data. As expected, adding second and third velocity points helps further improve the mean error primarily for the case closest to the wall. In all cases, the rms error was about 1.5% (not shown in this figure). The single-point results in Fig. 8 show the largest error (though, still a very low value) at the lowest probe location of $y = 50$ μm. We attribute this to the accuracy of the hot-wire velocity data that close to the wall and also the accuracy in knowing the actual wall location. We find it remarkable that a single velocity data point that is not necessarily very close to the wall, nor in the linear sublayer, is sufficient to obtain an accurate estimate of wall friction (the highest probe location of $y = 7$ mm spans the range $176 \leq y^+ \leq 1{,}000$ in the 70 profiles of Österlund database). This is perhaps not too surprising when the velocity data are accurate and the model profile is an accurate representation of the turbulent boundary layer.

3.3 Influence of boundary layer (κ, B) constants

Throughout this work, we have considered a fix set of the commonly-used boundary layer constants ($\kappa = 0.41$, $B = 5.0$). Over the last several years more refined estimates of these constants have been reported, ($\kappa = 0.38$, $B = 4.1$) based on zero pressure gradient flat-plate boundary layer data (Österlund et al. 2000), and ($\kappa = 0.42$, $B = 5.6$) based on superpipe data (McKeon et al. 2004). The approach and the results we have described here were not intended to address the question of which set of constants is the best to use. Considering our results are already producing a highly accurate estimate of wall shear (e.g. about 0.5% mean error in friction velocity), we conclude that the use of refined values of boundary layer constants would not have a practical consequence for the reported results and would at best lead to an improvement of about 0.5% in mean error for estimating the friction velocity. This general observation was, in fact, confirmed by recalculating the results of Fig. 6 using the constants ($\kappa = 0.38$, $B = 4.1$) instead. This observation also suggests that the estimate of wall shear based on the method we have described here is much less sensitive to the choice of the von Kármán constant κ than the Clauser method.

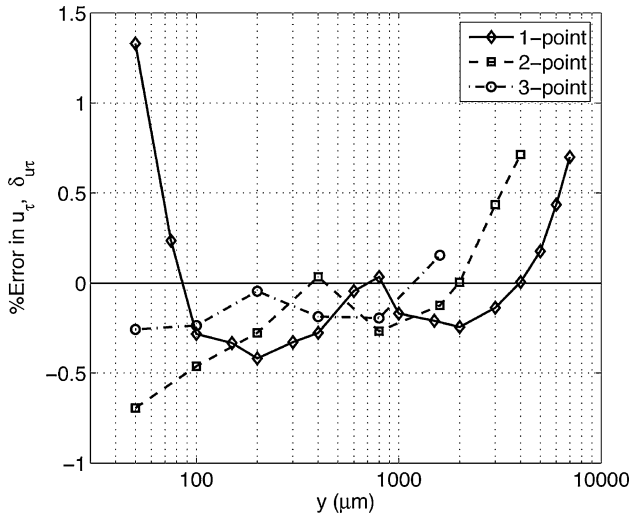

Fig. 8 Mean % error in friction velocity estimated from sparse data points selected from Österlund data (Musker profile, y_0 fixed at zero). Note that y locations are in physical units and % error is shown on an expanded scale. For multi-point cases, the location of the points are (y, $2y$) and (y, $2y$, $3y$)

4 Conclusions

We have presented a simple approach for estimating the wall friction in a turbulent boundary layer. The method utilizes the fit of the measured velocity data to a boundary layer model profile that extends the logarithmic profile all the way to the wall. A particular advantage of this method is that it can be used with velocity data that do not necessarily fall in the logarithmic region nor in the linear sublayer. As a result, the procedure can be easily automated without user intervention. Based on the tested data sets in zero pressure gradient and favorable pressure gradient boundary layers, we have shown that the new procedure can provide highly accurate estimates of the wall shear with a mean error of about 0.5% in friction velocity, or 1% in shear stress. This accuracy is shown to hold not only when many data points in a velocity profile are utilized, but also with very sparse measurements including only a single data point such as that originating from a near-wall probe. These results illustrate that it is possible to estimate based on mean velocity data the turbulent boundary layer wall friction with an accuracy comparable to that from independent direct measurements of wall-shear stress.

It is clear that the success of the approach we have presented relies on using a model profile that provides a sufficiently accurate representation of the turbulent boundary layer mean velocity profile. Between the two model profiles tested, the Musker profile performed much better than the Spalding profile. More refined model

profiles based on experimental data or DNS computations may lead to improvements over the results presented. In addition, as noted previously, the model profiles we have tested do not include the wake component of the full boundary layer profile, but can certainly be extended to incorporate appropriate models of the boundary layer wake component and this will extend the applicability of our approach to larger range of y^+_{max} values. The performance of such extended models has recently been presented, along with information on Reynolds number effects and choice of boundary layer constants (κ, B) (Chauhan et al. 2007). We note, however, that considering our results are already producing a highly accurate estimate of wall shear, we expect further refinements of the boundary layer model profile would have little influence on the reported results and would at best lead to an improvement of order 1% in the mean error for estimating the wall friction.

The approach we have presented here is expected to be useful for the estimation of wall friction in any turbulent boundary layer in which the profile in wall units collapses onto a common universal curve, which can be represented by a model profile with adequate accuracy. We may expect this includes turbulent boundary layers under favorable pressure gradient and those in adverse pressure gradient that are not too close to the separation point. It would be interesting to test the method presented here on turbulent boundary layers over a wide range of pressure gradients, both positive and negative, and different surface geometries in order to assess its range of usefulness. We note that the optimization procedure allows for independent determination of an uncertain wall location and it may be possible to use this procedure to also provide estimates of wall roughness.

Acknowledgments We thank Professor Hassan Nagib for providing us with the Österlund data set. The authors are grateful to Professor Donald Coles for discussions and many helpful suggestions.

References

Blackwelder R, Haritonidis J (1983) Scaling of the bursting frequency in turbulent boundary layers. J Fluid Mech 132:87–103

Chauhan KA, Nagib HM, Monkewitz PA, On the composite logarithmic profile in zero pressure gradient turbulent boundary layers, AIAA Paper No. AIAA 2007–532

Clauser FH (1956) The turbulent boundary layer. Adv Appl Mech 4:1–51

Coles DE (1968) The Young person's guide to the data. Computation of turbulent boundary layers, 1968 AFOSR-IFP Stanford Conference, vol. 2, Stanford University

Fernholz HH, Finley PJ (1996) The incompressible zero-pressure-gradient turbulent boundary layer: an assessment of the data. Prog Aerosp Sci 32:245–311

Fourguette D, Modarress D, Taugwalder F, Wilson D, Koochesfahani M, Gharib M, Miniature and MOEMS flow sensors, AIAA Paper No. AIAA-2001–2982

Fourguette D, Modarress D, Wilson D, Koochesfahani M, Gharib M, An optical MEMS-based shear stress sensor for high reynolds number applications, AIAA Paper No. AIAA-2003–0742

Kline SJ, Reynolds WC, Schraub FA, Runstadler PW (1967) The structure of turbulent boundary layers. J Fluid Mech 30:741–773

McKeon BJ, Li J, Jiang W, Morrison JF, Smits AJ (2004) Further observations on the mean velocity distribution in fully developed pipe flow. J Fluid Mech 501:135–147

Musker AJ (1979) Explicit expression for the smooth wall velocity distribution in a turbulent boundary layer. AIAA J 17:655–657

Ong L, Wallace JM (1998) Join probability density analysis of the structure and dynamics of the vorticity field of a turbulent boundary layer. J Fluid Mech 367:291–328

Österlund JM (1999), Experimental studies of zero pressure-gradient turbulent boundary-layer flow. Ph.D. thesis, Department of Mechanics, Royal Institute of Technology, Stockholm

Österlund JM, Johansson AV, Nagib HM, Hites MH (2000) A note on the overlap region in turbulent boundary layers. Phys Fluids 12:1–4

Spalart P (1988) Direct simulation of a turbulent boundary layer up to Re_θ = 1410. J Fluid Mech 187:61–98

Spalding DB (1961) A single formula for the Law of the Wall. J Appl Mech Trans ASME Ser E. 83:455

Wei T, Schmidt R, McMurtry P (2005) Comment on the Clauser chart method for determining the friction velocity. Exp Fluids 38:695–699

Zanoun E, Durst F, Nagib H (2003) Evaluating the Law of the Wall in two-dimensional fully developed channel flows. Phys Fluids 15:3079–3089